

EMANUELA GALLO¹⁾, GUADALUPE SÁNCHEZ-OLIVARES²⁾, BERNHARD SCHARTEL^{1),*}

Flame retardancy of starch-based biocomposites — aluminum hydroxide-coconut fiber synergy

Summary — The use of coconut fiber (CF) agricultural waste was considered as an environmentally friendly and inexpensive alternative in flame retarded biocomposites. To decrease the high content of aluminum trihydrate (ATH) required, the thermal decomposition (thermogravimetry), flammability [oxygen index (*LOI*) and UL 94 test] and fire behavior (cone calorimeter) of a combination of CF and ATH were investigated in a commercial blend of thermoplastic starch (TPS) and cellulose derivatives. CF induced some charring activity, slightly decreasing the fire load and burning propensity in cone calorimeter test. ATH decomposes endothermically into water and inorganic residue. Significant fuel dilution as well as a pronounced residual protection layer reduces the fire hazards. Replacing a part of ATH with coconut fibers resulted in improved flame retardancy in terms of ignition, reaction to small flame, and flame-spread characteristics [heat release rate (*HRR*), fire growth rate (*FIGRA*), *etc.*]. The observed ATH and CF synergy opens the door to significant reduction of the ATH contents and thus to interesting flame retarded biocomposites.

Keywords: biocomposites, flammability, starch, aluminum hydroxide, coconut fiber.

UNIEPALNIANIE BIOKOMPOZYTÓW NA BAZIE SKROBI — SYNERGIA WODOROTLENKU GLINU I WŁÓKIEN KOKOSOWYCH

Streszczenie — Badano możliwość zastosowania dodatku włókna kokosowego (CF), pochodzącego z odpadów rolniczych, jako tania i przyjazną dla środowiska alternatywną metodę uniepalniania biokompozytów. Wykonano próbki kompozytów skrobi termoplastycznej z dodatkiem środka uniepalniającego w postaci wodorotlenku glinu (ATH), CF lub ich mieszaniny (tabela 1). Określono parametry rozkładu termicznego otrzymanych próbek (rys. 1, tabela 2), zbadano ich palność wykonując test UL 94 (rys. 2, tabela 3) oraz wyznaczając wartości indeksu tlenowego (*LOI*) (tabela 3), a także wykonując pomiary za pomocą kalorymetru stożkowego (rys. 3–5, tabela 4). Uzyskane wyniki pozwoliły stwierdzić, że zarówno dodatek CF jak i ATH powodował ograniczenie palności badanych biokompozytów. Zauważono, że zastosowanie jako środka uniepalniającego mieszanki ATH i CF daje efekt synergiczny związany ze wzmocnieniem działania uniepalniającego w porównaniu z użyciem pojedynczego napełniacza. Zaobserwowany efekt daje możliwość ograniczenia, stosowanego zwykle w dużych ilościach, dodatku ATH, a jednocześnie uzyskania skuteczniej uniepalnionych biokompozytów.

Słowa kluczowe: biokompozyty, palność, skrobia, wodorotlenek glinu, włókno kokosowe.

INTRODUCTION

Natural fibers in composites are attractive alternative to conventional synthetic fibers such as glass or carbon fibers. The potential use of agricultural waste as an environmentally friendly and inexpensive approach to fibrous polymer reinforcement has long been well established [1, 2]. In tropical and subtropical regions, natural fibers from bamboo, coconut husk, sisal (agave) and

banana are abundant and relatively cheap. Plantations of coconut, in particular, are among the most abundant plantations in tropical countries worldwide. Once the fruit has been used for culinary purposes, the shell is normally discarded, raising major problems related to the long decay time and the amount of non-food waste produced. Lignocellulosic fibers extracted from the husk of nuts, known as coconut fibers (CF), may represent a key versatile candidate for eco-compatible composite materials [3]. Despite their tendency to form fiber aggregates during processing, their low resistance to moisture, variability of composition [4] and poor compatibility with hydrophobic matrix polymers [5], their use in reinforcement applications [6] was established successfully in polyester [7], polypropylene [8], rubber [9], and biodegradable polymers [10].

¹⁾ BAM Federal Institute for Materials Research and Testing, Unter den Eichen 87, 12205 Berlin, Germany.

²⁾ CIATEC, A.C. Center of Applied Innovation in Competitive Technologies, Omega No. 201, Fracc. Industrial Delta, León, 37545, Guanajuato, Mexico.

^{*}) Author for correspondence; e-mail: bernhard.schartel@bam.de

The wide commercialization of biopolymers is hampered by the competition from inexpensive commodity polymers as well as from engineering polymers that provide ambitious properties such as flame retardancy, both of which are already familiar to the customer. Thus the recent research has moved toward the use of inexpensive biodegradable polymers and composites from annually renewable crops and agro-industrial waste streams. Starch, an inexpensive and abundant product available annually from corn and other crops, is one of the most studied and promising matrices. In order to reduce drawbacks such as excessive hydrophilicity and brittleness, blends with other polymers are normally used.

In this work, a commercial blend of thermoplastic starch and cellulose derivatives was combined with natural coconut fibers. Whereas most of the literature usually looks at the mechanical reinforcement [11] of biocomposites, analogous to a few other papers [12–17], the main focus here was put on thermal decomposition and fire retardancy. In order to preserve the eco-friendly character of the composites, aluminum trihydroxide (ATH) was used as a well established flame retardant mineral filler [18]. Because of the high load of ATH normally needed to achieve satisfactory results in terms of fire behavior, the investigation was set up to find positive effects between the flame retardant and the natural fibers, allowing a reduction in the ATH content.

EXPERIMENTAL

Materials

Starch is an abundant, inexpensive, and annually renewable material available from potatoes as well as corn and other crops. It is composed of amylose, a mostly linear α -D-(1-4)-glucan and amylopectin, a branched α -D-(1-4)-glucan. Ratio of amylose and amylopectin varies with the starch source [19], and their variation provides a natural mechanism for regulating starch material properties. By mixing and blending starch with other polymers, its properties can be regulated easily and efficiently. A commercial blend made of thermoplastic starch and cellulose derivatives (designated TPS in the text) was purchased from Novamont (Italy) under the Mater-Bi[®] trademark. Mater-Bi[®] degradation degree of approximately 90 % was achieved in the controlled composting test according to ASTM D 5338. Grade YI01U was chosen as a biodegradable and compostable grade for rigid and dimensionally stable injection molded items, with mechanical properties and moldability close to those of polystyrene [20].

Coconut fibers (CF) as waste from the husk of the coconut fruit were obtained from Mexico Coir Industrial Company.

Aluminum trihydroxide (ATH) of 99.5 % purity, characterized by the surface area of 12 m²/g was used.

Sample preparation

The compounding of untreated CF with TPS and ATH, in amounts specified in Table 1, was carried out using a twin-screw counter-rotating extruder (Leistritz) with 7 zones ($L/D = 32$, extruder diameter 27 mm). The temperature profile was fixed according to the biopolymer technical data sheet and was set to 180/185/195/200/200/195/190 °C (from feed to die). The rotation speed was set to 50 rpm. All blends were dried under vacuum at 75 °C for 12 h before injection, due to the highly hygroscopic character of TPS. An injection molding machine (Milacron TM55) was used to prepare suitable samples for further investigation. The following injection temperature profile was 185/187/193/197 °C with the injection speed of 95 mm/s and pressure of 130 bar.

Table 1. Composition of investigated TPS biocomposites

Symbol of biocomposite	CF, phr	ATH, phr
TPS	—	—
TPS/CF	10	—
TPS/ATH	—	40
TPS/ATH/CF	10	30

Methods of testing

Thermal analysis was performed using a Netzsch-TG 209 ASC F1 Iris (Netzsch, Selb, Germany). Samples of 10 mg were heated in alumina pans from 30 to 900 °C at the heating rate of 10 °C/min under a constant nitrogen flow of 30 cm³/min. Blank measurements were performed to evaluate the apparatus-specific deviations including buoyant forces.

The flammability (reaction to a small flame) of the materials was determined by oxygen index (*LOI*) according to ISO 4589 (specimen: 127 × 6.5 × 3.2 mm) and UL 94 according to IEC 60695-11-10 (specimen: 127 × 12.7 × 3.2 mm). The fire behavior under forced-flaming conditions was assessed using a cone calorimeter (Fire Testing Technology, East Grinstead, UK) according to ISO 5660. External heat flux of 50 kWm⁻² was applied on the top of 100 × 100 × 3 mm plates, horizontally placed in an aluminum tray. All measurements were performed in triplicate and the results averaged.

RESULTS AND DISCUSSION

Pyrolysis

The thermal decomposition of TPS and its combination with CF and ATH under inert atmosphere of nitrogen is reported in Figure 1 and the results are summarized in Table 2. The decomposition profile for TPS was characterized by the begin of decomposition (2 % of mass

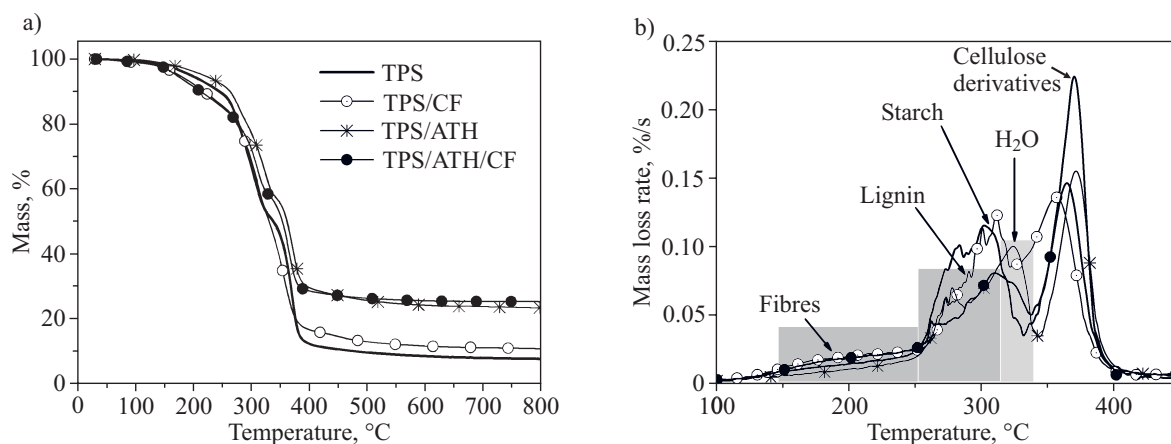


Fig. 1. Thermograms of TPS and its composites: a) mass loss, b) mass loss rate

loss) around 152 °C ($T_{2\%}$). Because of the lower thermal stability of lignocellulosic fibers [21, 22], $T_{2\%}$ was decreased by around 20 °C in TPS/CF. TPS/ATH/CF showed a similar temperature of beginning of decomposition (Table 2). An early mass loss was observed in all the materials between room temperature and 250 °C. Part of the mass loss observed during early decomposition of TPS was attributed to moisture desorption. In the same temperature range the hemicellulose component of CF underwent depolymerization (Fig. 1b) between 190 and 250 °C [22], increasing the mass loss of the early stage up to 15 %. The thermal profile of TPS was characterized by two main mass loss steps at temperatures with maximal mass loss rate 302 °C (DTG_{max1}) and 370 °C (DTG_{max2}), attributed to thermal decomposition of the starch and cellulose derivative, respectively [22, 23]. In all the fibers containing the formulation, lignin decomposition was observed as a broad peak throughout the range, decomposing between 280 and 500 °C [24]. An additional decomposition step at about 325 °C [25] was observed in TPS/ATH due to endothermic water release (Fig. 1b). TPS left a residue mass of around 7 %. The slightly increased mass of residue for TPS/CF proved the ability of the coconut fibers to contribute to carbonaceous charring. The 23 % of mass residue collected for TPS/ATH was related mainly to the formation of 20.5 wt. % of inorganic Al_2O_3 as a consequence of the endothermic dehydration. The expected residue mass formation for TPS/ATH/CF, considering an ATH content of 30 phr, was 15.4 %. The

detected amount of 21 % for TPS/ATH/CF characterized an inorganic carbonaceous residue.

In conclusion, lignocellulosic CF deteriorated TPS thermal stability by enhancing decomposition at lower temperatures. ATH decomposed endothermically into water and inorganic residue. Replacing part of ATH with coconut fibers did not significantly affect the thermal decomposition behavior with respect to decomposition temperatures, but increased the residue formation synergistically.

Table 2. Results of thermogravimetry investigations (under N_2 atmosphere, error ± 1 °C, ± 1.0 wt. %)

Symbol of biocomposite	TPS	TPS/CF	TPS/ATH	TPS/ATH/CF
Onset decomposition				
$T_{2\%}$, °C	152	136	166	141
Early mass loss (30–250 °C)				
Δ mass, wt. %	5.0	15.4	8.3	12.4
First mass loss				
Δ mass, wt. %	40.2	30.5	34.6	30.9
DTG_{max1} , °C	302	311	323	310
Second mass loss				
Δ mass, wt. %	47.5	38.3	29.5	30.2
DTG_{max2} , °C	370	356	371	364
Residue at 800 °C				
Mass, %	7.3	10.5	23.0	21.5

Table 3. Flammability test results

Symbol of biocomposite	TPS	TPS/CF	TPS/ATH	TPS/ATH/CF
LOI, %	18.2	20.4	24.0	24.7
UL 94 HB burning rate, mm/min	25.0	33.1	18.7	14.5
Visual observation	flaming and dripping	dripping (in vertical burning), no dripping (in horizontal burning), afterglow	no dripping	no dripping, afterglow
t_{igr} , s	23 \pm 2	24 \pm 2	34 \pm 2	38 \pm 2

Flammability and ignitability

The flammability (reaction to small flame) of various composite materials in terms of *LOI* and UL 94 test results are summarized in Table 3. The addition of only 10 phr of CF increased the *LOI* value in comparison to pure TPS from 18.2 to 20.4 %. This slight increase is remarkable, since fiber composites with such a filling grade often show the opposite behavior [26, 27]. The addition of 40 phr of ATH (28.6 wt. % in composite) to TPS increased the *LOI* value up to 24.0 %. Replacing 10 phr of ATH with 10 phr of CF in TPS/ATH/CF, resulted in *LOI* of 24.7 % and this *LOI* value is slightly larger than for TPS/ATH, which has the same amounts of all fillers but more ATH content. The *LOI* of TPS/ATH/CF corresponded to a superposition of the effect observed for ATH and CF, taking into account the reduced ATH content. Assuming that the *LOI* increase is less than a linear increase with ATH load [25], a slight synergistic performance was indicated for TPS/ATH/CF in *LOI*. The *LOI* of TPS/ATH/CF was clearly higher than expected for an ATH content of 30 phr (21.4 wt. % in composition).

None of the investigated materials passed the vertical burning UL 94 test because of intense burning, achieving only a UL 94 HB (horizontal burning) classification. Nevertheless some clear differences in burning behavior were detected. Both TPS and TPS/ATH showed high flammability, with intense dripping in vertical testing, consuming the sample up to the holding clamps. The dripping is suppressed by ATH in the horizontal setup. The use of CF in TPS/CF and TPS/ATH/CF affected the burning behavior: the samples no longer exhibited any dripping and showed a pronounced afterglow of the carbonaceous residue (Fig. 2). According to UL 94 HB test results (Table 3), CF is detrimental to the burning rate of TPS, showing a higher burning rate than TPS alone. The fibers prevented the reduction of material and heat in the pyrolysis zone through melt flow and dripping. ATH

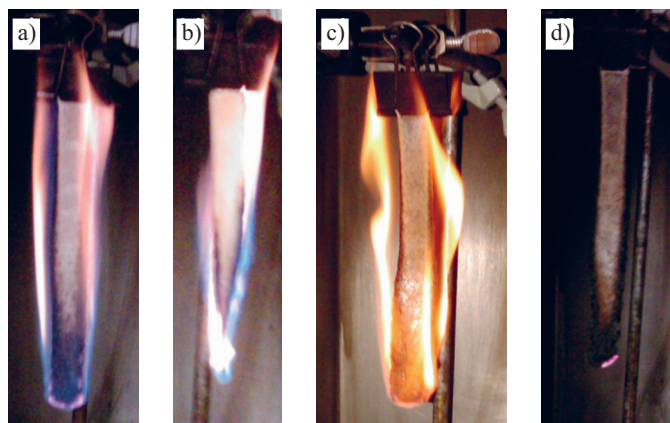


Fig. 2. Flammability in the vertical UL 94 burning test: a) TPS burning, b) TPS burning accompanied by melt flow and dripping, c) TPS/CF burning without dripping, d) TPS/CF afterglow

clearly reduced the burning rate, as expected. There was a remarkably strong synergistic effect when ATH and CF were combined in TPS/ATH/CF. Even though the ATH content was reduced and adding CF alone had a negative impact, the burning rate of TPS/ATH/CF is clearly lower than that for TPS/ATH. TPS/ATH/CF clearly showed the lowest burning rate, suggesting a synergy between ATH and CF as a promising approach to reduce the amount of ATH.

The influence on ignitability was monitored using the time to ignition (t_{ig}) from the cone calorimeter experiments. The t_{ig} value for TPS was 23 s and did not change with addition of CF beyond the margin of uncertainty. A clear increase in t_{ig} was achieved only in materials containing ATH. As already observed elsewhere [28], the endothermic dehydration and water release from ATH delayed ignition, as in TPS/ATH (Table 3). The replacement of ATH with CF showed a clear synergistic effect in t_{ig} . The t_{ig} value of TPS/ATH/CF was not only greater than expected for TPS/ATH with its smaller ATH content, but also clearly greater than the investigated TPS/ATH. Even though the amount of ATH was reduced and adding CF alone had no impact, the t_{ig} is largest for TPS/ATH/CF.

Fire behavior – visual observation

The fire behavior was investigated using cone calorimeter and the results are presented in Figure 3. TPS alone, once ignited, burned homogeneously and completely with a steady flame zone above the bubbling liquid surface until all the material was consumed and hardly any char was left. CF altered the combustion behavior of TPS. Ignition was followed by a first flaming stage characterized by anaerobic pyrolysis of the polymer and the simultaneous emergence of the surface layer (Fig. 3a). The surface layer rose, increasing rapidly in size until the end of fuel release, with strong surface glowing observed (afterglow) (Fig. 3b). Small flames and glowing over the surface were detected until the residue was completely consumed by thermo-oxidative phenomena.

In all materials containing ATH, a stable crust was formed even during the first stages of combustion. The formation of a surface layer of Al_2O_3 from ATH decomposition produced a compact white char acting as a shield to heat and mass transfer between the polymer and the flame [29, 30]. Strong surface deformation was observed in both TPS/ATH and TPS/ATH/CF until the char collapsed leaving a white crusty residue (Fig. 3).

Heat release rate and flame spread

The heat release rate (*HRR*) curves obtained under forced-flaming combustion for the investigated materials in cone calorimeter are reported in Figure 4. A strong increase in *HRR* was observed for TPS, exhibiting the typical profile of a rather thin non-charring material [31]. Within the range of uncertainty, the maximal value (peak)

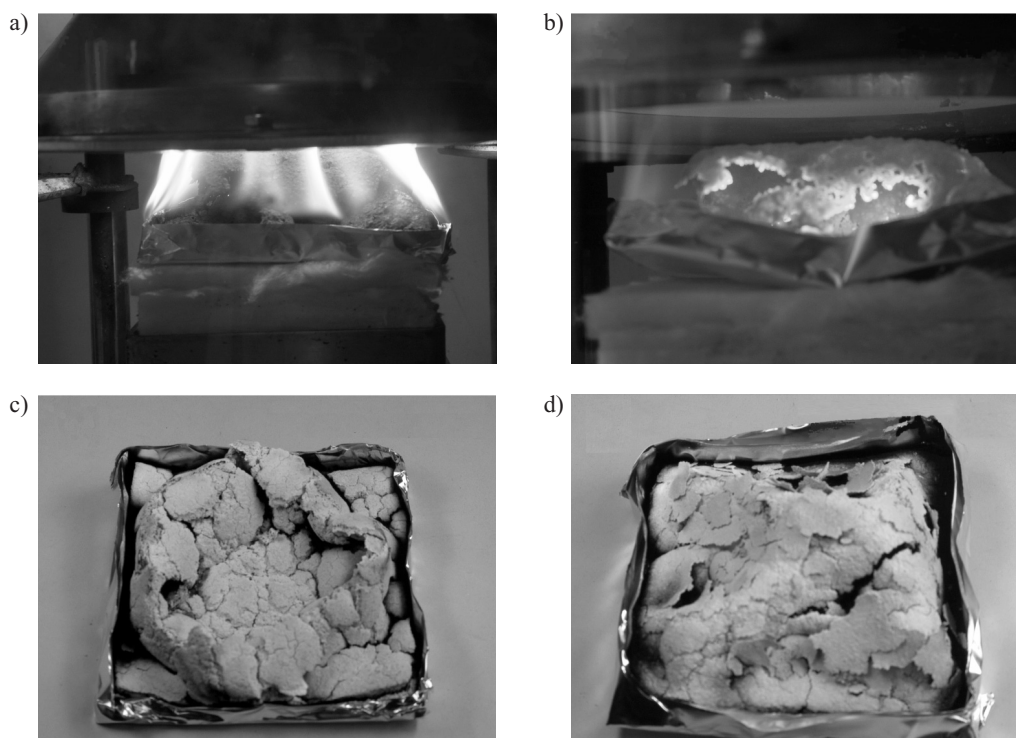


Fig. 3. Combustion behavior during cone calorimeter investigations of TPS/CF (a and b), and fire residues after the cone calorimeter test for TPS/ATH (c), and TPS/ATH/CF (d)

of *HRR* curve (*PHRR*) for TPS was not changed by the addition of CF (Table 4). Nevertheless the *HRR* pattern changed systematically through the addition of CF. After the same initial increase, the *HRR* value was reduced compared to the value observed for TPS, since the surface was now controlled by the residual layer. The formation of this surface layer results in a small but reproducible maximum in *HRR* followed by a decrease in *HRR*. However, this layer was not stable enough to prevent the *HRR* increase to the same level as for TPS towards the end of burning. The *HRR* pattern was also clearly altered by the addition of ATH. The initial increase in *HRR* value was delayed, as was already discussed in terms of t_{ig} . As a consequence of the protection layer formed, the *HRR*

curve showed the typical profile for a residue or char-forming material [31], resulting in a pronounced 45 % decrease in *PHRR* value. The residual protection layer is stable enough to maintain the protection layer effect over the whole test. The reduction of *HRR* was accompanied by a pronounced increase in the burning time. These results indicated an important protection mechanism at the surface [32] that hindered the mass or heat transport between the flame zone and pyrolysis. Replacing a part of ATH with CF in TPS/ATH/CF achieved a similar reduction in *PHRR* than in TPS/ATH even though the ATH content was reduced. The combination of ATH and CF showed a clear synergy with respect to *PHRR* reduction. The unaltered curve profile indicated no signifi-

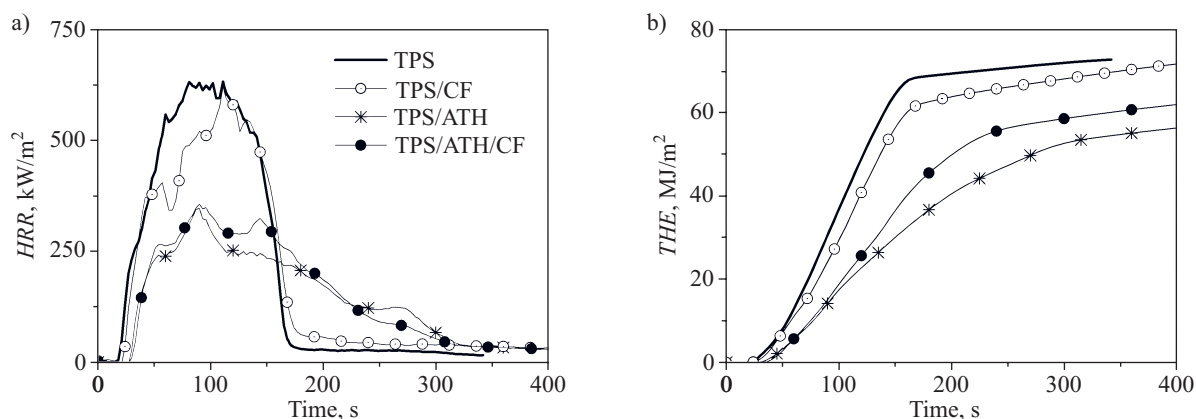


Fig. 4. Results of cone calorimeter measurements presenting time dependence of: a) heat release rate (HRR), b) total heat evolved (THE)

cant change in the fire mechanism or effectiveness of the residual protection layer.

In an attempt to rank the materials in terms of flame and fire growth, two different parameters were used, fire growth rate (*FIGRA*) and $PHRR/t_{ig}$ (Table 4). The propensity to cause a quickly growing fire was estimated by the *FIGRA* parameter, which has the greatest slope in the

of part of ATH with CF achieved a better *THE* value than expected from adding of 30 phr of ATH.

Table 4 shows the average residue amounts at flame-out and at the end of the test. The fire residues at flame-out corresponded roughly to the residues observed in thermogravimetry under nitrogen. In good approximation the stable flame is fed mainly by anaerobic

Table 4. Results of cone calorimeter investigation (irradiation 50 kW/m²)

	TPS	TPS/CF	TPS/ATH	TPS/ATH/CF
<i>PHRR</i> , kW/m ²	635 ± 50	587 ± 50	346 ± 50	352 ± 50
<i>FIGRA</i> , kW/(s · m ²)	5.7 ± 0.3	5.0 ± 0.3	3.9 ± 0.3	2.7 ± 0.3
<i>PHRR/t_{ig}</i> , kW/(m ² · s)	27.6 ± 0.5	24.1 ± 0.5	10.2 ± 0.5	9.2 ± 0.5
<i>THE</i> , MJ/m ²	74 ± 1	68 ± 1	51 ± 1	58 ± 1
<i>EHC</i> , MJ/(m ² · g)	1.60 ± 0.02	1.58 ± 0.02	1.36 ± 0.02	1.39 ± 0.02
Residue _{flame-out} , wt. %	6.3 ± 0.1	8.5 ± 0.1	15.3 ± 0.1	20.1 ± 0.1
Residue _{end} , wt. %	0.4 ± 0.1	1.3 ± 0.1	11.0 ± 0.1	9.6 ± 0.1

HRR curve versus time. A significant reduction in the *FIGRA* value for TPS/CF (30 % lower than for TPS), was due mainly to the shift in the *PHRR*, occurring at a later time when the fibers were added. The burning propensity of TPS/ATH and TPS/ATH/CF was in the same order of magnitude and corresponded to a reduction of around 50 % compared to TPS. In this case, the change in burning behavior, along with the reduced *PHRR*, was responsible for the reduction in the *FIGRA*. Since the *PHRR* and t_{ig} represent the two most important material characteristics controlling the flame spread, the *HRR* of the burning area and ease of ignition of the surrounding area, $PHRR/t_{ig}$ was also proposed as a reasonable empirical index for assessing cone calorimeter data with respect to fire growth phenomena [33]. A reduced propensity of *FIGRA* was observed in TPS/CF (~12 % less than for TPS). The addition of 40 phr of ATH to TPS reduced the fire growth value drastically (by ~60 %). Surprisingly, replacing a part of ATH with CF in TPS/ATH/CF affected the flame spread positively: the $PHRR/t_{ig}$ value obtained was not only clearly better than the expected effect of using 30 phr ATH, but also smaller than for TPS/ATH using 40 phr ATH. As it was expected from the ignition and *PHRR*, the replacement of ATH with CF showed very interesting synergistic effect on flame retardancy in the common indices used for fire growth and flame spread.

Total heat evolved, fire residue and effective heat of combustion

The total heat evolved (*THE*) profile as a measure of fire load is reported in Figure 4b. CF addition in TPS/CF reduced the *THE* by 8.1 % compared to the value for TPS (Table 4). About 30 % of *THE* reduction was achieved with the addition of ATH in TPS/ATH. The replacement

pyrolysis during burning. The inorganic-carbonaceous residue turns into a more inorganic residue at the end of the test through thermo-oxidation of the carbonaceous char during the afterglow. Addition of ATH to TPS in TPS/ATH and TPS/ATH/CF resulted in an increase in inorganic residue, corresponding to the conversion of some ATH into Al₂O₃ and the loss of the rest. Addition of CF increases the carbonaceous char at flame-out. The increase in carbonaceous char for TPS/ATH/CF was clearly higher than in TPS/CF. Indeed, the inorganic carbonaceous residue of TPS/ATH/CF was not only larger than what was expected of adding 30 phr of ATH, but also higher than the investigated TPS/ATH. A synergy in residue yield during pyrolysis becomes apparent.

In Table 4 the effective heat of combustion (*EHC*) of the volatiles is shown, evaluated as the *THE* to mass loss ratio of the sample. A change in the *EHC* is attributed to flame inhibition in the gas phase, dilution of the fuel by incombustible volatiles, or a decrease due to the release of products with a lower *EHC*. The 7 % reduction in the *EHC* achieved in TPS/CF in comparison to *EHC* of TPS was due to the release of different pyrolysis products with a lower heat of combustion. The water release due to ATH decomposition diluted the fuel and was responsible for the 30 % reduction in the *EHC*. Replacing a part of ATH with CF resulted again in *EHC* surprisingly close to the *EHC* of TPS/ATH with higher ATH content. This synergy may be explained by the increase in carbonaceous char accompanied by the reduction of carbon content in the pyrolysis products.

In conclusion, both CF and ATH worked mainly in the condensed phase. Due to water release cooling down the flame zone and diluting fuel, ATH showed a relevant gas phase mechanism as well. The charring of the CF decreased the amount of fuel and the burning propensity,

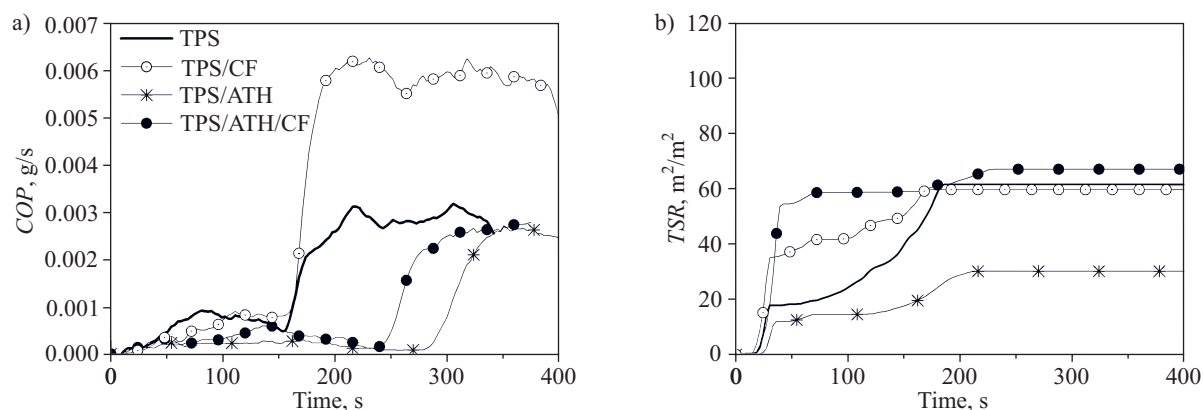


Fig. 5. Results of cone calorimeter measurements presenting the time dependence of: a) CO production (COP), b) total smoke release (TSR)

respectively. In combination with ATH the carbonaceous charring is increased synergistically, and thus also the residue amount, reducing the *EHC* of the volatiles and decreasing the fire load.

Smoke and CO production

Smoke release and carbon monoxide production were observed in the cone calorimeter investigations. The CO production (*COP*) and total smoke release (*TSR*) during burning of samples are shown in Figure 5. Considering that the ventilation conditions have a significant effect on the smoke and CO production, the data presented are always limited to a certain scenario [34]. After the first stage of flaming combustion (0–150 s), in which the pyrolysis of the condensed phase was essentially anaerobic, the *COP* profile (Fig. 5a) reached a minimum when flame-out occurred, followed by a thermo-oxidative regime characterized by oxidation of carbonaceous char. The afterglow was characterized by a much higher CO yield and thus *COP*. All of the investigated materials showed considerable afterglow after flame-out, which is the highest for TPS/CF. The *COP* of TPS/CF was twice than that of TPS. Apart from the shift in time to flame-out, adding ATH reduced the *COP* only slightly during afterglowing in TPS/ATH. Indeed TPS, TPS/ATH and TPS/ATH/CF showed very similar *COP* curves during afterglow. Compared to TPS/CF, the latter observation for TPS/ATH/CF indicated the synergistic effect on protection of carbonaceous char for the combination of ATH and CF. *TSR* curve is shown in Figure 5b. As expected, ATH functioned as a smoke suppressant [25]. The *TSR* of TPS/ATH was decreased by around 50 % compared to *TSR* of TPS. The smoke reduction was somewhat counterbalanced by the combination with coconut fibers.

CONCLUSIONS

The thermal decomposition and fire behavior of TPS in combination with CF and ATH were investigated. The lignocellulosic CF deteriorated the thermal stability of

TPS by increasing the mass loss at the beginning of decomposition. ATH decomposed endothermically into water and Al_2O_3 , diluting fuel and forming an inorganic residual protection layer. Replacing a part of ATH with CF did not significantly affect the thermal decomposition behavior, but showed a synergistic increase in inorganic-carbonaceous fire residue.

Even though all of the investigated materials scored only HB classification in the UL 94 test, the burning rates, *LOI* and t_{ig} show clear flame retardancy effects for adding ATH and CF as well as suppressing melt flow and dripping. The replacement of ATH and CF in part yields synergistic flame retardancy in burning tests, *LOI* and t_{ig} .

ATH formed an important protection layer during combustion under forced-flaming conditions, hindering the mass and heat transport between the flame zone and condensed phase. This resulted in a change in the *HRR* curve pattern and a significant decrease in all the fire characteristics (*PHRR*, total fuel release, *FIGRA*). Due to several synergistic effects (t_{ig} , residual protection layer, residue mass and *EHC*), promising results in terms of fire performance and burning propensity were obtained by replacing some of ATH with CF. The synergistic combination of ATH and CF opens the door to a reduction in the ATH content necessary to achieve flame retarded bio-composites.

REFERENCES

1. Bilba K., Arsene M. A., Ouensanga A.: *Bioresour. Technol.* 2007, **98**, 58.
2. Władyska-Przybylak M., Bujnowicz K., Kozłowski R., Rydarowski H.: *Przem. Chem.* 2008, **87**, 1172.
3. Schuh T., Gayer U.: „Automotive applications of natural fiber composites” in „Lignocellulosic-Plastics Composites” (Eds. Leão A. L., Carvalho F. X., Frollini E.), Unesp Publishers, Botucatu, Brazil 1997.
4. Satyanarayana K. G., Pillai C. K. S., Sukumaran K., Pillai S. G. K., Rohatgi P. K., Vijayan K.: *J. Mater. Sci.* 1982, **17**, 2453.
5. George J., Sreekala M. S., Thomas S.: *Polym. Eng. Sci.* 2001, **41**, 1471.

6. Carvalho K. C. C., Mulinari D. R., Voorwald H. J. C., Cioffi M. O. H.: *Bioresources* 2010, **5**, 1143.
7. Monteiro S. N., Terrones L. A. H., D'Almeida J. R. M.: *Polym. Test.* 2008, **27**, 591.
8. Leblanc J. L., Furtado C. R. G., Leite M. C. A. M., Visconte L. L. Y., Ishizaki M. H.: *J. Appl. Polym. Sci.* 2006, **102**, 1922.
9. Arumugam N., Selvy K. T., Rao K. V., Rajalingam P.: *J. Appl. Polym. Sci.* 1989, **37**, 2645.
10. Monteiro S. N., Terrones L. A. H., Lopes F. P. D., D'Almeida J. R. M.: *Rev. Mater.* 2005, **10**, 571.
11. Riedel U., Nickel J.: *Angew. Makromol. Chem.* 1999, **272**, 34.
12. Schartel B., Braun U., Schwarz U., Reinemann S.: *Polymer* 2003, **44**, 6241.
13. Fois M., Grisel M., Le Bras M., Duquesne S., Poutch F.: „Fire Retardant Polypropylene/Flax Blends: Use of Hydroxides” in „Fire Retardancy of Polymers: New Applications of Mineral Fillers” (Eds. Le Bras M., Wilkie C. A., Bourbigot S., Duquesne S., Jama C.), RSC, Cambridge 2005.
14. Kozłowski R., Władyka-Przybylak M.: *Polym. Adv. Technol.* 2008, **19**, 4463.
15. Gallo E., Schartel B., Acierno D., Russo P.: *Eur. Polym. J.* 2011, **47**, 1347.
16. Manfredi L. B., Rodriguez E. S., Władyka-Przybylak M., Vazquez A.: *Polym. Degrad. Stab.* 2006, **91**, 255.
17. Le Bras M., Duquesne S., Fois M., Grisel M., Poutch F.: *Polym. Degrad. Stab.* 2005, **88**, 80.
18. Hornsby P. R., Rotheron R. N.: „Fire Retardant Fillers for Polymers” in „Fire Retardancy of Polymers: New Applications of Mineral Fillers” (Eds. Le Bras M., Wilkie C. A., Bourbigot S., Duquesne S., Jama C.), RSC, Cambridge 2005.
19. Gross R., Kalra B.: *Science* 2002, **297**, 803.
20. Bastioli C.: *Polym. Degrad. Stab.* 1998, **59**, 263.
21. Albano C., Gonzalez J., Ichazo M., Kaiser D.: *Polym. Degrad. Stab.* 1999, **66**, 179.
22. Rosa M. F., Chiou B. S., Medeiros E. S., Wood D. F., Mattoso L. H. C., Orts W. J., Imam S. H.: *J. Appl. Polym. Sci.* 2009, **111**, 612.
23. Rosa M. F., Chiou B., Medeiros E. S., Wood D. F., Williams T. G., Mattoso L. H. C., Orts W. J., Imam S. H.: *Bioresour. Technol.* 2009, **100**, 5196.
24. Saheb N. D., Jog J. P.: *Adv. Polym. Technol.* 1999, **18**, 351.
25. Horn W. E.: „Inorganic Hydroxides and Hydroxycarbonates: Their Function and Use as Flame Retardant Additives” in „Fire Retardancy of Polymeric Materials” (Eds. Grand A. F., Wilkie C. A.), Marcel Dekker Inc., New York 2000.
26. Casu A., Camino G., de Giorgi M., Flath D., Laudi A., Morone V.: *Fire Mater.* 1998, **22**, 7.
27. Schartel B., Pötschke P., Knoll U., Abdel-Goad M.: *Eur. Polym. J.* 2005, **41**, 1061.
28. Braun U., Schartel B.: *Macromol. Chem. Phys.* 2004, **205**, 2185.
29. Schartel B., Weiß A.: *Fire Mater.* 2010, **34**, 217.
30. Wu G. M., Schartel B., Bahr H., Kleemeier M., Yu D., Hartwig A.: *Combust. Flame* 2012, **159**, 3616.
31. Lyon R. E.: „Plastics and rubber” in „Handbook of Building Materials for Fire Protection” (Ed. Harper C. A.), McGraw-Hill Handbooks, New York 2004.
32. Schartel B., Braun U.: *e-Polymers* 2003, No. 13.
33. Babrauskas V.: „Bench-scale methods for prediction of full-scale fire behavior of furnishings and wall linings”, SFPE Technology Report, Society of Fire Protection Engineers, Boston 1984.
34. Schartel B., Hull T. R.: *Fire Mater.* 2007, **31**, 327.

Received 26 IV 2012.

W kolejnym zeszycie ukażą się m.in. następujące artykuły:

- J. Ganster, J. Erdmann, H.-P. Fink — Biokompozyty (*j. ang.*)
- A. Jaskiewicz, A. K. Bledzki, P. Franciszczak — Właściwości mechaniczne kompozytów PLA wzmocnianych włóknami naturalnymi, włóknami regenerowanej celulozy lub włóknami szklanymi (*j. ang.*)
- A. Boczkowska, S. Awietjan — Inteligentne kompozyty magnetoreologiczne
- M. Barcikowski, W. Królikowski — Wpływ modyfikacji żywicy na udarność kompozytów poliestrowo-szklanych (*j. ang.*)
- K. Sałasińska, J. Ryszkowska — Stabilność wymiarowa, właściwości fizyczne, mechaniczne i cieplne kompozytów polietylenu dużej gęstości z łupinami orzecha ziemnego
- A. Lis, J. Laska — Wpływ dodatku montmorylonitu oraz nanorurek węglowych na odporność termiczną poli(metakrylanu metylu)
- W. Hufenbach, M. Gude, S. Geller, A. Czulak — Wytwarzanie kompozytów poliuretanowych wzmocnionych włóknami naturalnymi w procesie wtryskiwania z użyciem długich włókien (*j. ang.*)
- K. Czaplicka-Kolarz, D. Burchart-Korol, J. Korol — Ocena środowiskowa biokompozytów z zastosowaniem techniki LCA